

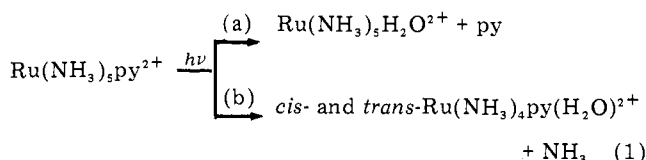
Photochemistry of the Ruthenium(II) Ammine Complexes, $\text{Ru}(\text{NH}_3)_5(\text{py-X})^{2+}$. Variation of Systemic Parameters to Modify Photochemical Reactivities¹

George Malouf and Peter C. Ford*²

Contribution from the Department of Chemistry, University of California, Santa Barbara, California 93106. Received April 1, 1977

Abstract: Quantum yields are reported for the photosolvation reactions of the ruthenium(II) complexes $\text{Ru}(\text{NH}_3)_5\text{py-X}^{2+}$ (where py-X is a substituted pyridine or related aromatic heterocycle) in aqueous solution and in the nonaqueous solvents dimethylformamide, dimethyl sulfoxide, and acetonitrile. Irradiation with visible light leads initially to excitation of metal to ligand charge transfer (MLCT) transitions; however, the excited state(s) responsible for photosolvation are proposed to have ligand field character. In this context, the series of $\text{Ru}(\text{NH}_3)_5\text{py-X}^{2+}$ complexes are categorized into "reactive" complexes, those with a ligand field state as the lowest energy excited state, and "unreactive" complexes, those with a lowest energy charge transfer excited state. In aqueous solution, the "reactive" complexes each display a MLCT maximum at wavelengths less than 460 nm and quantum yields for photosolvation of the pyridine (Φ_L) greater than 0.02 mol/einstein at each irradiation wavelength. The "unreactive" complexes have longer wavelength MLCT maximum and are as much as three orders of magnitude less photolabile when irradiated at these wavelengths. Thus it is demonstrated that variation of pyridine substituents alone can "tune" the energies of the MLCT state in a manner which leads to reversals in the order of the lowest energy excited states and to systematic variations in the photosubstitution quantum yields. Although quantum yields of "reactive" complexes are relatively independent of the photolysis wavelength, those of the "unreactive" complexes increase dramatically with decreasing λ_{irr} . Qualitatively, the reaction patterns noted in aqueous solution are also observed in the nonaqueous solvents. However, these patterns include two significant features. First, overall photolability is influenced by the identity of the solvent following the general order $\text{CH}_3\text{CN} > \text{H}_2\text{O} > \text{Me}_2\text{SO}$. Second, when the lowest MLCT and ligand field states are reasonably close in energy, a change in solvent may reverse the order of the lowest states, thus dramatically changing the reactivity pattern for that particular complex.

Previous studies in these laboratories have demonstrated that visible range photolysis of the d^6 complex $\text{Ru}(\text{NH}_3)_5\text{py}^{2+}$ in aqueous solution leads to ligand aquation³⁻⁵ (eq 1). This



complex ion displays an intense and broad absorption band with a λ_{max} of 407 nm which has been assigned as a metal to ligand charge transfer (MLCT) absorption.⁶ Formally, the MLCT excited state (MLCT*) can be visualized as having a Ru(III) center coordinated to the ligand radical anion (i.e., $(\text{NH}_3)_5\text{Ru}^{\text{III}}\text{py}^-$). However, since low spin d^5 Ru(III) ammine complexes are relatively unreactive toward ligand substitution, we have argued that the MLCT* is unlikely to be the direct precursor of the observed photoreaction and proposed a model in which a ligand field excited state (LF*) is responsible for ligand substitution.^{5,6} In this model (Figure 1), the reactive LF* is the lowest energy state of the electronic excited state manifold, and initial excitation into the MLCT state(s) is followed by efficient interconversion to this state. The rationales behind this proposition were as follows.

(1) The MLCT* is not expected to be substitution labile, especially toward NH_3 aquation.

(2) For Ru(II) ammine complexes not dominated by MLCT absorption in the electronic spectrum, LF bands are identifiable at wavelengths comparable to that of the $\text{Ru}(\text{NH}_3)_5\text{py}^{2+}$ MLCT band. For example, aqueous $\text{Ru}(\text{NH}_3)_6^{2+}$ displays a LF absorption (${}^1T_1 \leftarrow {}^1A_1$) at λ_{max} 390 nm (ϵ 39 $\text{M}^{-1} \text{cm}^{-1}$), $\text{Ru}(\text{NH}_3)_5\text{H}_2\text{O}^{2+}$ at λ_{max} 415 nm (43 $\text{M}^{-1} \text{cm}^{-1}$), and $\text{Ru}(\text{NH}_3)_5\text{CH}_3\text{CN}^{3+}$ at λ_{max} 350 nm (163 $\text{M}^{-1} \text{cm}^{-1}$).⁷ However, direct excitation into the LF states can only play a

very minor role for $\text{Ru}(\text{NH}_3)_5\text{py}^{2+}$ given the very large extinction coefficient of the MLCT band (7700 $\text{M}^{-1} \text{cm}^{-1}$).⁵

(3) Direct LF photolysis of systems displaying lowest energy LF absorption bands, namely, $\text{Ru}(\text{NH}_3)_6^{2+}$ and $\text{Ru}(\text{NH}_3)_5\text{CH}_3\text{CN}^{2+}$, leads to substitutional behavior ($\Phi \sim 0.2$ mol/einstein) in aqueous solution,^{7,8} consistent with the general observation that LF excitation of low spin d^6 complexes leads to substitutional processes for the heavier transition metals.⁶

(4) The quantum yields Φ_{py} for pyridine aquation from aqueous $\text{Ru}(\text{NH}_3)_5\text{py}^{2+}$ is essentially wavelength independent ($\Phi \sim 0.04$ mol/einstein) over the range 436–254 nm, thus suggesting interconversion of initially populated states to a common state.^{5,9}

The sensitivity of the MLCT bands of the $\text{Ru}(\text{NH}_3)_5(\text{py-X})^{2+}$ ions (where py-X is a substituted pyridine or related aromatic heterocycle) to parameters such as the substituent X or the solvent¹⁰ suggests ways to test the validity of the proposed model. LF state energies are generally insensitive to the solvent¹¹ and are relatively insensitive to pyridine substituents¹² in the electronically analogous rhodium(III) and cobalt(III) complexes $\text{M}(\text{NH}_3)_5(\text{py-X})^{3+}$. Therefore, it should be possible to use systematic variation of substituents and/or solvent to "tune"¹³ the MLCT energies to give cases where a charge transfer state is the lowest energy state. If the model is correct, these complexes should be relatively unreactive toward substitution. The studies described here are designed to test this excited state model, but they also serve to illustrate in general how systemic parameters such as structural or medium features may be objectively varied to modify the photochemical and/or photophysical properties of metal complexes. Understanding the consequences of such molecular perturbations is essential in the design of chemical systems for such practical applications as the conversion of radiant energy to chemical potential energy.¹⁴

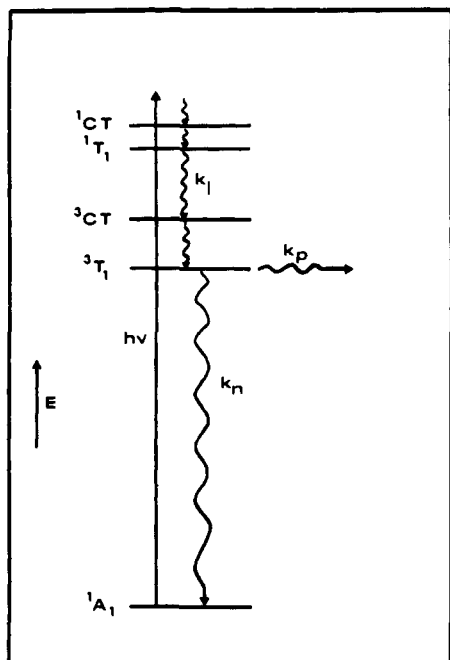


Figure 1. Proposed excited state diagram for the photoaquation of $\text{Ru}(\text{NH}_3)_5\text{py}^{2+}$. k_p represents reactions leading to photoproducts, k_n represents nonradiative deactivation.

Experimental Section

Materials. The recrystallized $[\text{Ru}(\text{NH}_3)_5(\text{py-X})][\text{BF}_4]_2$ salts were prepared from $[\text{Ru}(\text{NH}_3)_5\text{Cl}]\text{Cl}_2$ according to published procedures.^{5,10} Aqueous solutions for photolyses were prepared from redistilled water with reagent sodium chloride used to maintain ionic strength. The dimethylformamide, dimethyl sulfoxide, and acetonitrile used as solvents were redistilled before use. All solutions were deaerated with argon which had been passed sequentially through a chromous bubbler, a drying column, then a gas washing bottle filled with the appropriate solvent. Reinecke's salt used in actinometry was purchased from Eastman as $(\text{NH}_4)[\text{Cr}(\text{NH}_3)_2(\text{SCN})_4]$ and converted to the potassium salt by recrystallizing from KNO_3 solution.

Spectra of several tetraamine complexes *cis*- and *trans*- $\text{Ru}(\text{NH}_3)_4(\text{L})\text{S}^{2+}$, $\text{L} = \text{NH}_3$, isonicotinamide (*isn*), or pyridine (*L*); $\text{S} =$ water, acetonitrile, dimethyl sulfoxide, or dimethylformamide, were obtained in the solvent *S* from compounds prepared in the following manners. (a) $\text{Ru}(\text{NH}_3)_5\text{S}^{2+}$: a weighed sample (~ 30 mg) of freshly prepared $[\text{Ru}(\text{NH}_3)_5\text{H}_2\text{O}][\text{PF}_6]_2$ was dissolved in 50 mL of the appropriate deaerated solvent and the electronic spectrum was recorded immediately with a Cary 14 spectrophotometer. The various solvent species were not isolated. (b) *trans*- $\text{Ru}(\text{NH}_3)_4\text{pyS}^{2+}$: A 100-mg sample of $[\text{trans-Ru}(\text{NH}_3)_4\text{SO}_4\text{py}]\text{Cl}$ in deaerated 0.1 M H_2SO_4 was reduced over $\text{Zn}(\text{Hg})$. Addition of saturated $(\text{NH}_4)\text{PF}_6$ solution leads to the precipitation of $[\text{trans-Ru}(\text{NH}_3)_4(\text{py})\text{H}_2\text{O}](\text{PF}_6)_2$ which was isolated, washed, and dried. Spectra were obtained from solutions prepared by dissolving weighed samples of the aquo complex (~ 17 mg) in 50 mL of the appropriate, deaerated solvent. (c) *cis*- $\text{Ru}(\text{NH}_3)_4(\text{py})\text{S}^{2+}$: A 45-mg sample of $[\text{cis-Ru}(\text{NH}_3)_4(\text{py})\text{Cl}]\text{Cl}_2$ in 0.1 M H_2SO_4 was reduced over $\text{Zn}(\text{Hg})$. Addition of saturated NaClO_4 solution gave solid $[\text{cis-Ru}(\text{NH}_3)_4(\text{py})\text{H}_2\text{O}][\text{ClO}_4]_2$ which was isolated and dried. Spectra were obtained by dissolving weighed samples of this material in measured volumes of the appropriate solvents. (d) Spectra were obtained for the *cis* and *trans* species $\text{Ru}(\text{NH}_3)_4(\text{isn})\text{S}^{2+}$ in an analogous fashion.

Photolysis Procedures. Monochromatic irradiations at 405, 433, 449, 479, 500, 520, or 546 nm were carried out using a 150-W xenon lamp in an Oriol Model 6110 Universal Arc Lamp source with Oriol or Balzer interference filters for monochromatization at the appropriate wavelengths. The interference filters had an average band pass of 10 nm, and the collimated beam intensities ranged from 2.2×10^{-8} to 5.6×10^{-8} einstein $\text{s}^{-1} \text{cm}^{-2}$ as determined by Reinecke ion actinometry. Samples were photolyzed in 10-cm path length fused silica cells held in a thermostated cell holder. Aqueous reaction solutions were made up in pH 3/0.2 M NaCl, but photolyses in nonaqueous

solvent contained no salt or acid other than the complexes of interest ($\sim 2 \times 10^{-5}$ M). All solutions were deaerated by entraining with argon prior to photolysis and were stirred during irradiation. The photo-reactions were monitored spectrally on a Cary 14 spectrometer and quantum yields for substitution of *py-X* were calculated from decreases in the MLCT band intensity as described previously.^{5,7} In each case, corrections were made for dark reactions (generally very minor) occurring under analogous conditions. Ammonia aequation quantum yields (eq 1b) were evaluated by a procedure described by Hintze.^{7,8} Aqueous photo solutions were 0.2 M NaCl, pH 4 (10^{-4} M HCl), $\sim 1 \times 10^{-3}$ M of the ruthenium complex, and 0.1 M acetonitrile. The deaerated solution was photolyzed to approximately 10% reaction in a thermostated 2-cm cell (25 °C). Simultaneously dark reaction was carried out with an identical solution. Subsequent to the photolysis, the pH of the dark and irradiated solutions were determined, and quantum yields for acid consumption were calculated from the pH differences. Quantum yields for ligand substitution in nonaqueous solvents were evaluated from spectral data as described below.

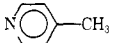

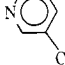
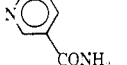
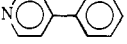
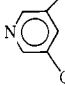

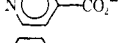

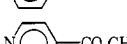



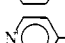
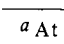
Results

(1) **Studies in Aqueous Solution.** The MLCT λ_{max} of $\text{Ru}(\text{NH}_3)_5\text{py-X}^{2+}$ is sharply dependent on the substituent *X*. Visible range photolysis causes decreases in the charge transfer absorption band intensity, and spectral consequences of the photochemical reactions of $\text{Ru}(\text{NH}_3)_5\text{py}^{2+}$ are described elsewhere.^{5,7,9} In the 0.2 M Cl^- solution, oxidation of $\text{Ru}(\text{II})$ to $\text{Ru}(\text{III})$ with competitive aequation of *py-X* or NH_3 would be detected by optical density increases at ~ 330 nm indicating the formation of chlororuthenium(III) complexes. Since no such increases were observed for any of the photolyses reported here in carefully deaerated solutions, $\text{Ru}(\text{II})$ oxidation must represent at most a small fraction of the disappearance of the MLCT absorption^{7,9} (vide infra). An upper limit $\Phi_{\text{ox}} < 10^{-3}$ has been determined for the 366-nm photolysis of aqueous $\text{Ru}(\text{NH}_3)_5\text{CH}_3\text{CN}^{2+}$, and a similar value for photooxidation would be expected with the pyridine complexes.^{5,7}

Pyridine photoaquation is the principal pathway responsible for decreases in the MLCT absorptions of aqueous $\text{Ru}(\text{NH}_3)_5\text{py}^{2+}$. Competing ammonia aequation produces the tetraammine ions $\text{Ru}(\text{NH}_3)_4(\text{H}_2\text{O})\text{py}^{2+}$ which have MLCT maxima and extinction coefficients very similar to those of the starting complex. Thus, for this complex the spectroscopic quantum yields $\Phi_{\text{L}}(\text{spec})$ exceed the actual quantum yields for eq 1a by at most 10–15% owing to the contributions of eq 1b. Similar spectral patterns are observed for the $\text{Ru}(\text{NH}_3)_4(\text{H}_2\text{O})\text{isn}^{2+}$ isomers and in the ensuing discussion it is assumed that these patterns are consistent for the other *py-X* complexes studied in aqueous solution. However, unlike the pyridine system, some of these complexes show greater ammonia aequation quantum yields (Φ_{NH_3}) than for *py-X* aequation. Thus, in these cases, a significant error may result from the assumption that $\Phi_{\text{L}}(\text{spec})$ accurately reflects the aequation of *py-X* since this value is calculated with the assumption that NH_3 aequation has no spectral consequence. Nonetheless, since loss of NH_3 from the coordination sphere also leads to OD decreases at the MLCT λ_{max} of the starting material, the $\Phi_{\text{L}}(\text{spec})$ values represent upper limits for the aequation quantum yield of *L*, and, in conjunction with Φ_{NH_3} values measured independently, serve to establish photoreaction patterns for the series of *py-X* complexes.

Quantum yields $\Phi_{\text{L}}(\text{spec})$ for the various $\text{Ru}(\text{NH}_3)_5\text{py-X}^{2+}$ complexes are summarized in Table I. In each case listed, the photolysis wavelength λ_{irr} was approximately equal to the charge transfer maximum, $\lambda_{\text{max}}(\text{CT})$. Those complexes where $\lambda_{\text{max}}(\text{CT})$ is less than ~ 460 nm display $\Phi_{\text{L}}(\text{spec})$ values in the range 0.02–0.05 mol/einstein while those having $\lambda_{\text{max}}(\text{CT})$ exceeding ~ 460 nm are much less photoactive toward aequation of *L*. The range of $\Phi_{\text{L}}(\text{spec})$ values spans three orders of magnitude, and those complexes with the lower energy charge transfer maxima are the least photoreactive. Also, the

Table I. Spectroscopic Quantum Yields for the Photoaquation of $\text{Ru}(\text{NH}_3)_5\text{L}^{2+}$ in Aqueous Solution^a


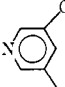
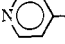





$\text{Ru}(\text{NH}_3)_5\text{L}^{2+} + \text{H}_2\text{O} \xrightarrow{h\nu} \text{Ru}(\text{NH}_3)_5\text{H}_2\text{O}^{2+} + \text{L}$				
L	λ_{max} (CT), nm	ν_{max} (CT), μm^{-1}	λ_{irr} , nm	$\Phi_{\text{L}}(\text{spec}) \times 10^3$, mol/einstein
	398	2.51	405	37 ± 3 (2) ^b
	407	2.45	405	45 ± 2 (3) ^b
	426	2.35	436	48 ± 2 (2) ^b
	427	2.34	433	8.5 ± 0.2 (4)
	446	2.24	449	33 ± 1 (3)
	447	2.24	449	42 ± 2 (4)
	454	2.20	455	22 ± 5 (2)
	457	2.19	460	26 ± 3 (4) ^c
	472	2.12	479	1.4 ± 0.1 (4) ^d
	4.79	2.09	479	1.07 ± 0.04 (4)
	497	2.01	500	0.27 ± 0.03 (3) 0.25 ± 0.04 (4) ^e
	523	1.91	520	0.25 ± 0.06 (3) 0.26 ± 0.02 (4) ^e
	529	1.89	520	0.11 ± 0.02 (4) ^f
	540	1.85	540	0.04 ± 0.01 (2)
	545	1.83	546	0.05 ± 0.01 (3)

^a At 25 °C. In pH 3 aqueous NaCl solution (0.2 M) except where noted. Average deviation and number of independent determinations (in parentheses) listed. ^b Reference 5. ^c pH 10. ^d pH 7. ^e 1 M HCl. ^f 0.1 M HCl.

methyl isonicotinate ($\text{X} = 4\text{-CO}_2\text{CH}_3$) and 4-acetylpyridine ($\text{X} = 4\text{-COCH}_3$) complexes give the same quantum yields in 1.0 M HCl solution as in the pH 3, 0.2 M NaCl solutions; thus, thermal back reaction to form starting material is not significant in the overall photoreaction.

Comparison of the quantum yields in Table I suffers from the fact that λ_{irr} is also a variable of the accumulated data. For this reason, a number of the complexes were examined over ranges of photolysis wavelength to determine whether λ_{irr} would significantly influence $\Phi_{\text{L}}(\text{spec})$. These data are summarized in Table II. A previous study⁹ demonstrated that the photolysis of $\text{Ru}(\text{NH}_3)_5\text{py}^{2+}$ (λ_{max} 407 nm) gave only small variation in Φ_{py} (0.038–0.051) over the λ_{irr} range 254–436 nm. Similarly, the complexes of 3,5-dichloropyridine (λ_{max} 447 nm) and 4-phenylpyridine (λ_{max} 446 nm) display $\Phi_{\text{L}}(\text{spec})$ values relatively insensitive to λ_{irr} over the range 405–500 nm. The only systematic trend in each case is a modest increase in $\Phi_{\text{L}}(\text{spec})$ at the longer wavelengths. In contrast the complexes of isonicotinamide (λ_{max} 479 nm, $\text{X} = 4\text{-CONH}_2$), methyl isonicotinate (λ_{max} 497 nm, $\text{X} = 4\text{-CO}_2\text{CH}_3$), and 4-acetylpyridine (λ_{max} 523 nm) each display $\Phi_{\text{L}}(\text{spec})$ values which vary markedly with λ_{irr} over the range 405–520 nm. In each case

Table II. Quantum Yields in Aqueous Solution as a Function of Irradiation Wavelength for the Reaction

L	λ_{irr}	$\Phi_{\text{L}} \times 10^3$, mol/einstein ^a	$\Phi_{\text{NH}_3} \times 10^3$, mol/einstein ^b	$\Phi_{\text{TOT}} \times 10^3$, mol/einstein ^c
	366	43 ± 2		
	405	45 ± 2	63 ± 5	108
	436	51 ± 2		
	449	49 ± 1	63 ± 1	112
	405	38 ± 1	33 ± 1	71
	449	42 ± 2	19 ± 1	61
	479	43 ± 1		
	500	48 ± 2	17 ± 1	65
	405	31 ± 2	41 ± 2	72
	449	33 ± 1	19 ± 2	52
	500	37 ± 2	22 ± 2	59
	405	4.5 ± 0.1	22 ± 2	27
	449	1.5 ± 0.1		
	479	1.07 ± 0.04	5.3 ± 0.2	6.4
	500	0.37 ± 0.02	2.4 ± 0.1	2.8
	520	0.35 ± 0.02		
	546	0.30 ± 0.02	0.7 ± 0.1	1.0
	479	1.4 ± 0.1	1.8 ± 0.2	3.2
	405	4.7 ± 0.2		
	449	1.3 ± 0.1		
	479	0.72 ± 0.03		
	500	0.27 ± 0.02		
	405	4.5 ± 0.7	27 ± 1	32
	449	1.4 ± 0.1	8.6 ± 0.5	10
	520	0.25 ± 0.06	0.9 ± 0.1	1.2
	546	0.04 ± 0.01	$<0.8 \pm 0.2$	<0.84
	546	0.05 ± 0.01	0.05 ± 0.03	0.10

^a At 25 °C, in pH 3 aqueous NaCl solution (0.2 M). Average deviation, data for a minimum of three independent determinations in each case. ^b At 25 °C, in pH 4 solution as described in the Experimental Section. Average deviations listed for duplicate, independent determinations. ^c $\Phi_{\text{TOT}} = \Phi_{\text{L}} + \Phi_{\text{NH}_3}$.

the higher energy photolysis leads to greater quantum yields.

The effect of temperature on $\Phi_{\text{L}}(\text{spec})$ was briefly investigated for the 3,5-dichloropyridine and isonicotinamide analogue, and the respective apparent activation energies are 3.7 and 6.8 kcal/mol for 500 nm photolysis at 23 and 59 °C.

The spectroscopic technique does not provide any information regarding ammonia photoaquation from the $\text{Ru}(\text{NH}_3)_5\text{L}^{2+}$ complexes. For this reason, Φ_{NH_3} was monitored by pH changes of the acidic (pH 4.0) photolysis solution,^{7,9} since each equivalent of NH_3 released neutralizes 1 equiv of acid. When necessary, corrections were made for the pH changes due to the neutralization of photoaquated py-X.¹⁵ The Φ_{NH_3} values (Table II) display two features of particular note. First, on a qualitative scale the Φ_{NH_3} values follow a pattern similar to the $\Phi_{\text{L}}(\text{spec})$ values reported above. Complexes with the shorter wavelength charge transfer maxima are the more photoreactive and their Φ_{NH_3} and Φ_{TOT} ($\Phi_{\text{NH}_3} + \Phi_{\text{L}}(\text{spec})$) values are much less wavelength dependent than those complexes having $\lambda_{\text{max}}(\text{CT})$ greater than ~460 nm (Figure 2). Second, several of the latter complexes show NH_3 aquation to be the dominant pathway.

(2) **Studies in Nonaqueous Solvents.** Spectroscopic quantum yields $\Phi(\text{spec})$ for photolyses in the nonaqueous solvents DMF, Me_2SO , and CH_3CN are listed in Table III. These are calculated according to an assumption similar to that used for the spectroscopic quantum yield calculations in aqueous solution,

Table III. Quantum Yields $\Phi(\text{spec})$ for $\text{Ru}(\text{NH}_3)_5\text{py-X}$ in Various Aprotic Solvents

L	$\lambda_{\text{max}}(\text{CT}),^a$			$\Phi(\text{spec}) \times 10^3^b$	L	$\lambda_{\text{max}}(\text{CT}),^a$			$\Phi(\text{spec}) \times 10^3^b$	
	nm	$\lambda_{\text{irr}}, \text{nm}$	$\lambda_{\text{mon}}, \text{nm}$			nm	$\lambda_{\text{irr}}, \text{nm}$	$\lambda_{\text{mon}}, \text{nm}$		
In Dimethyl Sulfoxide Solution					Isonicotinamide					
Pyridine	447	405	447	48 ± 1	501	405	501	3.9 ± 0.5		
		449		44 ± 1				449	1.6 ± 0.2	
		500		35 ± 1				500	0.54 ± 0.05	
3,5-Cl ₂ py	491	405	491	7.8 ± 0.1	520	520		0.39 ± 0.01		
		449		5.1 ± 0.1						
		500		2.1 ± 0.2						
4-Ph-py	497	405	497	16 ± 1	In Acetonitrile Solution					
		447		8.7 ± 0.1	Pyridine	407	365	407	140 ± 10	
		500		3.5 ± 0.1			450	450	170	
		546		1.6 ± 0.1			405	407	150 ± 10	
449	4.7 ± 0.1	449	407	180						
Isonicotinamide	511	405	511	10.5 ± 0.3	449	449	449	140 ± 10		
		449		4.7 ± 0.1				450	160	
		479		2.8 ± 0.2				449	122 \pm 3	
		500		1.2 ± 0.2				468	62 \pm 3	
		520		0.77 ± 0.03						
4-Acetyl-py	566	405	566	9.8 ± 0.7	449	449	449	67		
		449		3.3 ± 0.3				460	52 ± 1	
		520		0.22 ± 0.02				490	57	
		546		0.08 ± 0.01				520	41 ± 2	
								490	46	
In Dimethylformamide Solution					4-Acetyl-py	504	405	504	15.5 ± 0.5	
Pyridine	436	405	436	36 ± 3					540	41
		433		41 ± 1					500	5.2 ± 0.1
		449		43 ± 1					540	6.0
3,5-Cl ₂ -py	482	405	482	5.1 ± 0.1					577	504
		449		4.9 ± 0.2	540	2.4				
		479		3.9 ± 0.2	540	9.2 ± 0.2				
		500		2.7 ± 0.1	523	11				
		520		2.2 ± 0.1	520	2.0 ± 0.1				
4-Ph-py	487	405	487	5.8 ± 0.2	523	449	523	0.82 ± 0.03		
		479		4.0 ± 0.1				550	1.0	
		520		3.1 ± 0.1				546	0.32 ± 0.03	
								577	0.39	

^a MLCT maxima in respective solvents. ^b 25 °C, in noted solvent with no added salts except the indicated complex in concentrations less than 10^{-4} M. $\Phi(\text{spec})$ is calculated with assumption that each photochemical event decreasing absorbance at λ_{mon} leads to complete bleaching at that wavelength. Each $\Phi(\text{spec})$ represents mean of at least three independent determinations with listed uncertainties representing the average deviations. λ_{mon} in each case is the $\lambda_{\text{max}}(\text{CT})$ in the appropriate medium except for some $\Phi(\text{spec})$ values for acetonitrile solution where wavelengths longer than $\lambda_{\text{max}}(\text{CT})$ were used. In these cases $\Phi(\text{spec})$ is calculated from the overall reaction corrected for extrapolation to 0% photolysis. ^c 95% acetonitrile/5% H₂O.

namely, that the photochemical processes being monitored lead to complete bleaching of the MLCT absorption band. This would be true if the sole photoreaction were the solvolytic displacement of py-X from $\text{Ru}(\text{NH}_3)_5\text{py-X}^{2+}$ since the solvent pentaammine complexes $\text{Ru}(\text{NH}_3)_5\text{S}^{2+}$ are essentially transparent in the visible wavelength region used to monitor the photoreaction (Table IV). However, given the importance of NH₃ photosubstitution in aqueous solution, such an assumption is unwarranted, and the spectra of the tetraammine complexes *cis*- and *trans*- $\text{Ru}(\text{NH}_3)_4(\text{py-X})\text{S}^{2+}$ in the respective solvents (Table IV) need to be considered to understand the significance of the $\Phi(\text{spec})$ values.

Me₂SO Solution. The spectra of the various Me₂SO complexes lead to the least ambiguous interpretations of the $\Phi(\text{spec})$ values. Replacement of an ammonia (either *cis* or *trans* to the aromatic heterocycle) by a Me₂SO ligand leads to very large blue shifts of the MLCT maxima with resultant nearly complete bleaching of the absorbance at the MLCT λ_{max} of the pentaammine complex (Table IV). Thus, since every photosubstitution event (replacement of py-X or *cis* or *trans* ammonia) leads to virtual complete bleaching at the monitoring wavelength, $\Phi(\text{spec})$ in Me₂SO solution represents the total quantum yield for ligand substitution, i.e., $\Phi(\text{spec})$

= Φ_{TOT} . In this solvent, quantum yields for the pyridine, isonicotinamide, and 4-acetylpyridine complexes parallel the behavior for each of these complexes in water, although in each case Φ_{TOT} in Me₂SO is about one-third that in water. More striking differences, however, are seen for the 3,5-dichloropyridine and 4-phenylpyridine complexes. In contrast to the behavior in water the Φ_{TOT} values for these species are both much smaller in Me₂SO (more than the factor of one-third seen for the other complexes) but also are markedly dependent on λ_{irr} in a manner similar to that seen for the isonicotinamide and 4-acetylpyridine complexes.

DMF Solution. The spectra of the potential NH₃ substitution products in DMF lead to less definitive interpretation of $\Phi(\text{spec})$ measurements. Although photosubstitution of py-X causes nearly complete bleaching of the MLCT band, replacement of NH₃ by DMF gives spectra approximating that of the starting complex (Table IV). Thus one is tempted to conclude that $\Phi(\text{spec})$ simply reflects Φ_{L} ; however, small extinction coefficient differences between the pentaammine and tetraammine species could lead to significant errors in assuming that $\Phi(\text{spec}) = \Phi_{\text{L}}$ without an independent method of evaluating NH₃ substitution. As a consequence, the $\Phi(\text{spec})$ data reported for the reactions in DMF are somewhat am-

biguous; these very likely reflect the Φ_L s, but insufficient information is available to quantify this conclusion. Notably, in DMF the $\Phi(\text{spec})$ values (Table III) for the pyridine and isonicotinamide complexes are quantitatively very close to the $\Phi_L(\text{spec})$ values of the respective complexes in water (Table II). Thus the pyridine values are essentially independent of λ_{irr} while the isonicotinamide values are very much a function of the irradiation wavelength. However, $\Phi(\text{spec})$ values for the 4-phenylpyridine and 3,5-dichloropyridine complexes are much smaller and somewhat more wavelength dependent than those measured in aqueous solution.

Acetonitrile Solution. The spectral data for the ammonia substitution products in acetonitrile lie somewhat between the DMF and Me_2SO cases. Coordination of the π acceptor CH_3CN ligand blue shifts the MLCT band leaving a much smaller extinction coefficient at the wavelength corresponding to the pentaammine λ_{max} (Table IV). However, the extinction coefficient differences between $\text{Ru}(\text{NH}_3)_5\text{L}^{2+}$ and the NH_3 substitution products are not sufficient to give an unambiguous spectral analysis at this wavelength, so longer wavelengths where the ratios of the starting material and ammonia substitution product ϵ 's are larger (>5) were utilized for the calculation of $\Phi(\text{spec})$. At these wavelengths $\Phi(\text{spec})$ can be considered to reflect Φ_{TOT} , although such an assumption may underestimate Φ_{TOT} by as much as 15–20% if labilization of NH_3 is the predominant photochemical pathway. However, this potential error is minor in comparison to the other effects noted in the various solvent systems (vide infra).

In acetonitrile the quantum yields Φ_{TOT} are consistently larger than the respective Φ_{TOT} values measured under analogous conditions in aqueous solution, but for most of the complexes these parallel the values seen in water. For example, Φ_{TOT} for the pyridine complex is relatively high and is independent of λ_{irr} . Also, the 4-acetylpyridine and 4-formylpyridine complexes are much less photoactive and show λ_{irr} dependent quantum yields (Table III). The one exception is the isonicotinamide complex which is markedly more photoactive in acetonitrile than in the other solvents with Φ_{TOT} about one-third that for the pyridine complex and only marginally λ_{irr} dependent. Consequently for 520 nm irradiation $\text{Ru}(\text{NH}_3)_5\text{isn}^{2+}$ is an order of magnitude more photolabile in acetonitrile than in water.

Discussion

Aqueous Solution. The data in Tables I and II support certain aspects of the excited state model proposed for the pyridine complex (Figure 1).^{1b,5} The major features of this model are that initial MLCT excitation is followed by efficient interconversion to a lowest energy, spectrally unobservable, ligand field state and that net photoaquation of py and NH_3 are among the deactivation pathways of this state. With one exception (when $\text{X} = 3\text{-CONH}_2$)^{1b} each complex displaying a charge transfer maximum at wavelengths less than approximately 460 nm (i.e., $E(\lambda_{\text{max}}) \gtrsim 2.17 \mu\text{m}^{-1}$) is relatively active ($\Phi_L(\text{spec})$ 0.02–0.05, $\Phi_{\text{TOT}} > 0.05$ mol/einstein) toward photoaquation when irradiated in pH 3 aqueous solution at wavelengths approximating $\lambda_{\text{max}}(\text{CT})$. Complexes with $\lambda_{\text{max}}(\text{CT})$ at wavelengths longer than 460 nm are dramatically less photoactive toward aquation of L when irradiated at their $\lambda_{\text{max}}(\text{CT})$. Qualitatively, Φ_{TOT} follows a similar pattern, although the relative contributions of Φ_L and Φ_{NH_3} vary with the substituent X. These observations support the view that the modification of MLCT* energies with ligand substituents can reverse the excited state order to give a substitution unreactive charge transfer state with lowest energy. On the basis of this model, the complexes listed in Table I can be divided into two categories: “reactive” complexes being those with $\lambda_{\text{max}}(\text{CT}) < \sim 460$ nm and presumably having a lowest energy LF state;

Table IV. Spectral Properties of $\text{Ru}(\text{NH}_3)_5\text{py}^{2+}$, $\text{Ru}(\text{NH}_3)_5\text{isn}$. Possible Photoreaction Products in Nonaqueous Solvent(s)

Complex	λ_{max}^a (log ϵ) ^b	λ_{mon}^c (log ϵ) ^b
In Dimethylformamide		
$\text{Ru}(\text{NH}_3)_5\text{py}^{2+}$	436 (3.88)	436 (3.88)
$\text{Ru}(\text{NH}_3)_5\text{DMF}^{2+}$	423 (2.34)	436 (2.28)
<i>trans</i> - $\text{Ru}(\text{NH}_3)_4(\text{py})\text{DMF}^{2+}$	438 (4.03)	436 (4.03)
<i>cis</i> - $\text{Ru}(\text{NH}_3)_4(\text{py})\text{DMF}^{2+}$	429 (3.92)	436 (3.90)
$\text{Ru}(\text{NH}_3)_5\text{isn}^{2+}$ ^d	501 (4.10)	501 (4.10)
<i>trans</i> - $\text{Ru}(\text{NH}_3)_4(\text{isn})\text{DMF}^{2+}$	500 (4.11)	501 (4.11)
<i>cis</i> - $\text{Ru}(\text{NH}_3)_4(\text{isn})\text{DMF}^{2+}$	496 (4.03)	501 (4.03)
In Dimethyl Sulfoxide		
$\text{Ru}(\text{NH}_3)_5\text{py}^{2+}$	447 (3.89)	447 (3.89)
$\text{Ru}(\text{NH}_3)_5\text{DMSO}^{2+}$	317 (2.40)	447 (0.78)
<i>trans</i> - $\text{Ru}(\text{NH}_3)_4(\text{py})\text{Me}_2\text{SO}^{2+}$	325 (3.70)	447 (1.95)
<i>cis</i> - $\text{Ru}(\text{NH}_3)_4(\text{py})\text{Me}_2\text{SO}^{2+}$	344 (3.68)	447 (2.26)
$\text{Ru}(\text{NH}_3)_5\text{isn}^{2+}$	511 (4.12)	511 (4.12)
<i>trans</i> - $\text{Ru}(\text{NH}_3)_4(\text{isn})\text{Me}_2\text{SO}^{2+}$	369 (3.70)	511 (2.26)
<i>cis</i> - $\text{Ru}(\text{NH}_3)_4(\text{isn})\text{Me}_2\text{SO}^{2+}$	380 (3.62)	511 (2.30)
In Acetonitrile		
$\text{Ru}(\text{NH}_3)_5\text{py}^{2+}$	407 (3.83)	407 (3.83)
$\text{Ru}(\text{NH}_3)_5\text{CH}_3\text{CN}^{2+}$	354 (2.18)	450 (3.32)
<i>trans</i> - $\text{Ru}(\text{NH}_3)_4(\text{py})\text{CH}_3\text{CN}^{2+}$	378 (3.99)	407 (1.65)
<i>cis</i> - $\text{Ru}(\text{NH}_3)_4(\text{py})\text{CH}_3\text{CN}^{2+}$	375 (3.85)	450 (1.00)
$\text{Ru}(\text{NH}_3)_5\text{isn}^{2+}$	468 (4.08)	407 (3.68)
<i>trans</i> - $\text{Ru}(\text{NH}_3)_4(\text{isn})\text{CH}_3\text{CN}^{2+}$	428 (3.94)	450 (3.49)
<i>cis</i> - $\text{Ru}(\text{NH}_3)_4(\text{isn})\text{CH}_3\text{CN}^{2+}$	430 (3.86)	407 (3.53)
		450 (2.48)
		468 (4.08)
		490 (3.97)
		468 (3.60)
		490 (3.23)
		468 (3.56)
		490 (3.23)

^a λ_{max} in nm of longest wavelength absorption band. ^b $\text{M}^{-1} \text{cm}^{-1}$.

^c Wavelength used in monitoring photoreaction to calculate $\Phi(\text{spec})$ (Table III). ^d isn = isonicotinamide.

“unreactive” complexes being those with $\lambda_{\text{max}}(\text{CT}) > \sim 460$ nm presumably having a lowest energy MLCT*.¹⁶ It is worth emphasizing, however, that while the “unreactive” complexes may be less reactive with regard to ligand photosubstitution, complexes having lowest energy MLCT states may be active in photoredox processes.⁶ For example, the pyrazine complex $\text{Ru}(\text{NH}_3)_5\text{pz}^{2+}$, which is “unreactive” toward photosubstitution, has been shown¹⁷ to display electron transfer photochromism when photolyzed in aqueous solution with cupric ion.

The quantum yield data in Table I involve two simultaneous variables, $\lambda_{\text{max}}(\text{CT})$ and λ_{irr} (which was chosen to approximate closely $\lambda_{\text{max}}(\text{CT})$). While variation of λ_{irr} should not influence quantum yields if deactivation from upper states to the lowest energy excited state were 100% efficient, it is clear from Table II that photoaquation quantum yields are quite dependent on λ_{irr} for many of the systems studied here. In fact, the patterns for Φ_{TOT} and $\Phi_L(\text{spec})$ suggest another criterion for differentiating the “reactive” and “unreactive” complexes. Quantum yields for complexes in the “reactive” category are relatively independent of λ_{irr} , although some differences are noted in the ratios of pyridine aquation to ammonia aquation. In sharp contrast, $\Phi_L(\text{spec})$ and Φ_{TOT} values for the “unreactive” complexes are strongly wavelength dependent with order of magnitude decreases between the shorter and longer irradiation wavelengths of the ranges studied (Figure 2). Nonetheless, for every λ_{irr} studied, Φ_L for each “reactive” complex is larger than Φ_L for any “unreactive” complex (Tables I and II). These observations are consistent with the most important feature of the excited state model, i.e., the identities and characteristic

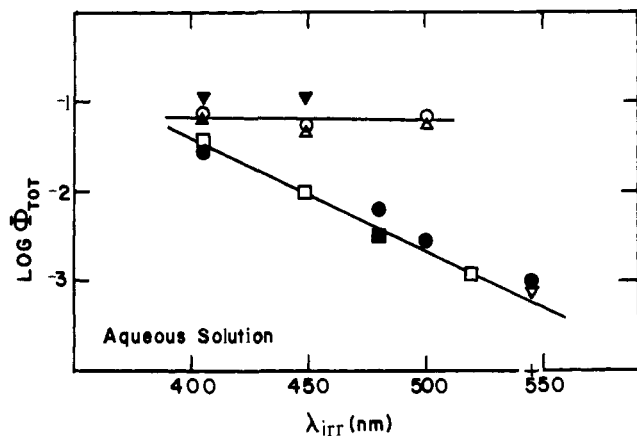


Figure 2. Wavelength dependence of $\log \Phi_{TOT}$ for the photolysis of $Ru(NH_3)_5L^{2+}$ in aqueous solution. Symbols for various L's: ∇ , pyridine; \circ , 3,5-dichloropyridine; Δ , 4-phenylpyridine; ∇ , methylpyrazinium; \bullet , isonicotinamide; \blacksquare , pyrazine; \square , 4-acetylpyridine. Lines drawn for illustrative purposes only.

reactivities of the lowest excited state(s). However, it is clear that (at least for the "unreactive" systems) interconversion to a common, presumably lowest energy, state does not occur with 100% efficiency.

Figures 3a and 3b represent modifications of the initial model and illustrate the proposed excited state orders for the "reactive" and "unreactive" complexes, respectively. Manifolds of the charge transfer and ligand field states are represented in recognition of the number of such states present. Under C_{2v} symmetry, there are 12 nondegenerate LF single and triplet states (6 each) which can be envisioned as the result of $t_{2g} \rightarrow e_g$ type one-electron promotion. Similarly, previously analysis¹⁰ of the MLCT absorptions of the pyridine complexes noted the possibility of a number of states as the consequence of spin allowed $\pi_d \rightarrow \pi_L^*$ promotion. Consideration of spin orbit coupling adds considerable complexity to the MLCT* manifold.¹⁸ To a first-order approximation, mixing of the MLCT and LF states is not allowed; therefore, the excited state manifolds have differentiable characters describable by their respective orbital parentages.

The key unknown detail of the system would be the approximate energy of the lowest LF* states. Attempts in this laboratory to observe the luminescence of the $Ru(NH_3)_5py^{2+}$ ion at temperatures as low as 18 K have so far proved unsuccessful; thus direct observation of states potentially important to the photochemistry has not yet proved viable. The MLCT absorption bands are quite broad.¹⁰ For example, the point on the long wavelength tail corresponding to 5% of the absorbance at the λ_{max} occurs at $\sim 0.4 \mu m^{-1}$ lower energy than $\lambda_{max}(CT)$. If we arbitrarily pick this as representing absorption directly into the lowest MLCT*, then the crossover from "reactive" to "unreactive" behavior which occurs for $\lambda_{max}(CT) = \sim 460$ nm ($2.17 \mu m^{-1}$) would suggest that the lowest LF thexi state should have an energy of $\sim 1.77 \mu m^{-1}$. Given the large energy differences between the singlet and triplet states of analogous Rh(III) ammine complexes,¹² we would be inclined to predict lowest LF triplets in the Ru(II) complexes to be $0.1-0.2 \mu m^{-1}$ lower than $1.77 \mu m^{-1}$. However, this discrepancy may reflect only the paucity of any direct information regarding the actual energies of lowest LF* and MLCT* states for any of these systems.

In Figure 3a it is assumed that initial excitation into the MLCT* manifold is followed by relatively efficient interconversion to the lowest energy LF* state from which deactivation pathways lead to aquation products or to the starting complex. The present data do not provide much information regarding the pathway by which the initial excitation travels from the

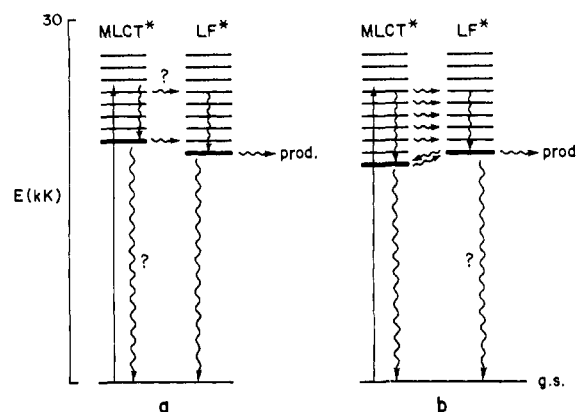
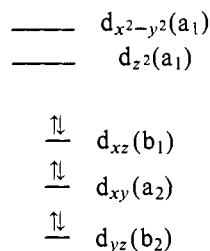


Figure 3. Revised excited state model for the photosolvation quantum yields. (a) Diagram for a "reactive" complex; (b) diagram for an "unreactive" complex.

MLCT* to the LF* manifolds. However, given the conclusions that states of $d\pi-\pi^*$ parentage communicate better with states of the same orbital parentage than with states of $d-d$ parentage,¹⁹ a reasonable pathway would be relatively efficient deactivation to the lowest MLCT* followed by crossing into the LF* manifold. To be efficient, the last step need not be competitive with $MLCT^* \rightarrow MLCT^*$ interconversions but must be more rapid than nonradiative deactivation to the ground state. The relative wavelength independence of the quantum yields for the "reactive" complexes implies more efficient interconversion to a common state (e.g., the lowest MLCT*), although the changes noted in the Φ_L/Φ_{NH_3} ratios with λ_{irr} for several "reactive" complexes do suggest the possible role of some upper excited states, presumably LF* in character.

The character of the lowest energy ligand field excited state can be analyzed qualitatively by examining the d orbital splitting expected under the C_{2v} symmetry imposed by the pyridine and the magnitude of $d\pi-p\pi$ back-bonding for these Ru(II) complexes.¹⁰ Pyridine is a somewhat weaker σ donor than NH_3 but is a π acceptor; therefore, the d orbital splitting pattern can be represented qualitatively by



The lowest state derived from a one-electron promotion would be the 3B_1 representing the electronic configuration $(d_{yz})^2(d_{xy})^2(d_{xz})^1(d_{z^2})^1$. The σ antibonding character of the d_{z^2} orbital suggests z axis labilization from such a state,^{12,20} a suggestion consistent with the pyridine aquation as a major pathway. Ammonia aquation is also consistent with z axis labilization; however, limited data suggest that ammonia aquation is not stereospecific.⁵ An absence of stereospecificity may be due to the interaction of other LF states but could also result from stereomobility in the photoaquation pathways. Analogous rhodium(III) complexes $Rh(NH_3)_5py \cdot X^{3+}$ have lowest energy LF states identifiable in both the absorption and emission spectra. However, these complexes display aquation of the unique ligand exclusively.¹² The differences between Ru(II) and Rh(III) no doubt are a reflection of the much greater π -bonding interactions between the Ru(II) and unsaturated organic ligands (vide infra).

For the "unreactive" complexes, Figure 3b suggests that the

initial excitation into the MLCT manifold is followed by deactivation to the lowest MLCT* competitive with crossing into the LF* manifold. The increasing values of Φ_{TOT} , Φ_L (spec), and Φ_{NH_3} with decreasing λ_{irr} is consistent with several interpretations: first, that higher energy LF states are more labile than lower energy members of the LF* manifold; second, that the higher energy irradiation increases the probability of crossing into the LF* manifold relative to deactivation to the lowest MLCT*; third, that at the shorter wavelengths, a larger percentage of the light absorbed results in the direct excitation into the LF* manifold. These explanations are not mutually exclusive.

The question remains whether the low yield photoaquation observed for long wavelength irradiation of the "unreactive" complexes represents reaction modes directly from the lowest MLCT* (perhaps due to some second-order mixing of LF and MLCT character) or thermal back population into the LF* manifold from lower energy MLCT states. A clear discrimination between these alternatives cannot be made with the current data; however, the fact that the relative roles of NH_3 vs. pyridine aquation is approximately independent of λ_{irr} for each "unreactive" complex (Table II) supports the latter alternative. Also the larger E_{app} for the "unreactive" isonicotinamide complex compared to the "reactive" 3,5-dichloro complex at the same λ_{irr} is consistent with a required thermal activation to give the LF* state from the MLCT* state (another explanation would simply be a greater energy barrier to aquation from the MLCT* state). Lastly, Φ_L continues to fall off for increasing $\lambda_{max}(CT)$ suggesting greater separation of the lowest LF and MLCT states with strongly electron-withdrawing groups.

It is interesting that several of the complexes categorized as "unreactive" show NH_3 aquation as the overwhelmingly major photolabilization pathway. The reasons for the predominance of this pathway for the 4-acetylpyridine and isonicotinamide complexes and its lesser importance for other complexes is not clear. These patterns of ligand photolability very likely are a function of the residual π bonding between the Ru^{II} center and the π -unsaturated ligand in the reactive LF* excited state and possibly of different admixtures of d_{z^2} and $d_{x^2-y^2}$ population in the relevant excited states.

Nonaqueous Solutions. In Me_2SO solution the MLCT absorption bands of the $Ru(NH_3)_5L^{2+}$ species are shifted to lower energy by about 40 nm relative to aqueous solution (Table III), and quantum yields for photosolvation Φ_{TOT} are generally smaller. The latter result is not surprising given that changing the solvent medium should influence a variety of kinetics parameters, particularly the nonradiative processes leading to the formation of ligand substitution products or to deactivation. However, the quantum yield data for the five complexes investigated in Me_2SO show a particularly interesting pattern. The pyridine, isonicotinamide, and 4-acetylpyridine complexes qualitatively parallel their photochemical behavior in aqueous solution. Thus, the pyridine complex is relatively photoactive with quantum yields rather independent of the excitation energy, while the other two systems are significantly less photoactive with λ_{irr} dependent quantum yields. In other words, the general criteria which allowed the categorization of the pyridine complex as "reactive" when photolyzed in aqueous solution and the other two as "unreactive" apparently are applicable in Me_2SO . In this context it is particularly interesting that the photoreactivities of the 3,5-dichloropyridine and 4-phenylpyridine complexes in Me_2SO do not parallel their reactions in aqueous solution. In Me_2SO both of these complexes are much more like the "unreactive" complexes than like the pyridine complex (Figure 4).

The 3,5-dichloro- and 4-phenylpyridine complexes each have MLCT maxima in aqueous solution (447 and 446 nm, respectively) close to the low energy end of the "reactive" range.

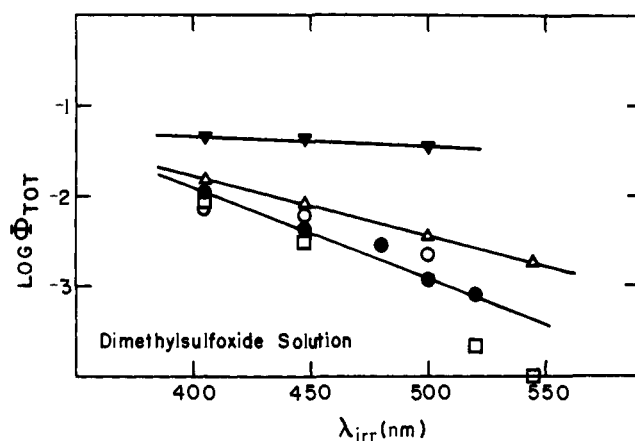


Figure 4. Wavelength dependence of $\log \Phi(\text{spec})$ for the photolysis of $Ru(NH_3)_5L^{2+}$ in Me_2SO solution. Symbols as in Figure 2.

Thus the significant decreases in $\Phi(\text{spec})$ and much greater dependence on λ_{irr} strongly suggest that the ~ 40 nm red shift in going from aqueous to Me_2SO solution leads to a change in the character of the lowest excited state from LF* to MLCT* for each of these cases.

Qualitatively, the quantum yield data obtained for the various complexes in DMF solution parallel the major trends seen in Me_2SO . The best comparison is between the $\Phi(\text{spec})$ values in DMF (Table III) and the $\Phi_L(\text{spec})$ values measured in water (Table II). Despite the ambiguity in interpreting $\Phi(\text{spec})$ in DMF (vide supra), it is noteworthy that the $\Phi(\text{spec})$ values for the pyridine and isonicotinamide complexes in DMF correspond very closely to the $\Phi_L(\text{spec})$ values measured in H_2O , while both the 3,5-dichloropyridine and 4-phenylpyridine complexes are much less photoactive in DMF and show much greater dependence of $\Phi(\text{spec})$ on λ_{irr} . Since the MLCT maxima in DMF are shifted ~ 30 nm to the red from their positions in aqueous solution, it again may be argued that changing the solvent medium has perturbed the excited state order to give a lowest energy MLCT* in these two cases.

In acetonitrile the MLCT maxima of $Ru(NH_3)_5(py-X)^{2+}$ are unshifted or are shifted to somewhat higher energies from their positions in aqueous solution. Although the quantum yields Φ_{TOT} are consistently larger than the respective values measured in aqueous solution, the general patterns are similar to those seen in other solvents. Thus the pyridine complex again demonstrates a reaction pattern consistent with a lowest energy LF state (i.e., a "reactive" complex) while the patterns for 4-acetylpyridine and 4-formylpyridine complexes are consistent with a lowest energy, relatively substitution inert MLCT state (i.e., "unreactive" complexes). However, the isonicotinamide complex which displays a $\lambda_{max}(CT)$ 10 nm higher energy than in water is much more photoactive than in any other solvent. This and the low sensitivity of Φ_{TOT} to λ_{irr} (Figure 5) suggest that the isonicotinamide complex has moved from the "unreactive" category to the "reactive" category in acetonitrile although showing some intermediate character. In other words, it appears that going from aqueous to acetonitrile solution modifies the excited state order to give a case where a reactive LF* state is below or comparable in energy to the lowest MLCT* state.

Comparisons of Solvent Systems. Variation of solvent introduces several major perturbations. One of these, the solvent induced shifts in $\lambda_{max}(CT)$ (Table III), might result from changes in the MLCT excitation state energies or from Franck-Condon factors. Similar solvent shifts of MLCT bands have been noted for the tungsten and molybdenum carbonyl complexes, $M(CO)_4phen$ and $M(CO)_4bipy$.²¹ In addition, one might expect the solvent to affect the rates of nonradiative deactivation or of the ligand substitution step. The latter per-

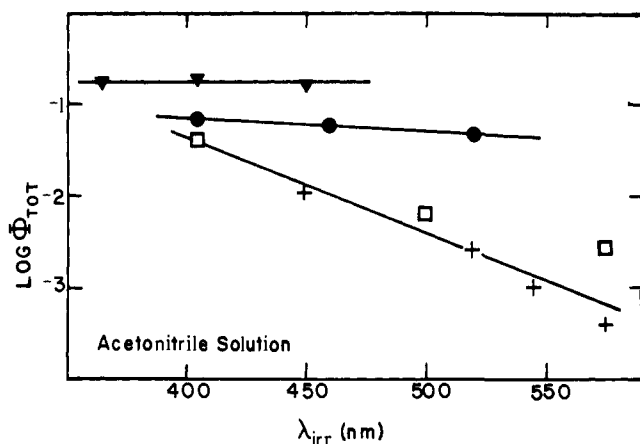


Figure 5. Wavelength dependence of $\log \Phi(\text{spec})$ for the photolysis of $\text{Ru}(\text{NH}_3)_5\text{L}^{2+}$ in acetonitrile solution. Symbols as in Figures 2 and 4 except that $+$ = 4-formylpyridine. $\Phi(\text{spec})$ values plotted are those obtained by monitoring wavelengths longer than the respective $\lambda_{\text{max}}(\text{CT})$ values (see Table III).

turbation might be the result of differences in the nucleophilicity of the incoming solvent molecule or conceivably of effects on cage recombination processes. The accumulated data for solvent effects on photosolution reactions do not clearly indicate general trends. For example, quantum yields for the LF excitation of $\text{Co}(\text{CN})_6^{3-}$ have been shown to be insensitive to solvent characteristics such as dielectric constant or the nature of the solvent's coordinating atom.^{11c} Within experimental uncertainty, reactions in H_2O , acetonitrile, DMF, ethanol, and pyridine each gave the same Φ_{CN^-} . However, a recent study of the photoreactions of $\text{trans-Cr}(\text{NH}_3)_2(\text{SCN})_4^-$ has shown that the photosubstitution reactions of this ion are sensitive to the solvent medium.²² In the present case, these factors may each influence the quantum yields observed for various $\text{Ru}(\text{NH}_3)_5\text{py-X}^{2+}$ complexes where the general order of photoreactivity (Φ_{TOT}) in the various solvents is $\text{CH}_3\text{CN} > \text{H}_2\text{O} > \text{Me}_2\text{SO}$.

From a broad overview, the model for "reactive" and "unreactive" complexes offered in Figure 3 has general validity with regard to the photoreactions in each of the solvents. However, the use of various solvents does offer the possibility of "tuning" the charge transfer excited states to lower energies as in DMF or Me_2SO or to higher energies as in acetonitrile while the energies of LF states are likely to be little perturbed by the solvent medium. Although solvent effects on the photochemistry of several transition metal complexes have been studied,^{11c,22-26} to our knowledge the cases described here represent the first examples of metal complexes where the solvent induced perturbations in photoreactivity can be attributed to reversals in the energy ordering of the lowest excited states.

From a more detailed viewpoint, the solvent effects on the overall photoreactivity are easily accommodated by the model described since this model placed no specific restrictions on effects of substituents or external perturbations on the relative roles of respective deactivation pathways. The variation in Φ_{TOT} values for the "reactive" pyridine complex in the different solvents suggests the possibility of an associative photosubstitution mechanism rather than the commonly assumed dissociative pathway for the LF excited states of d^6 complexes. An alternative explanation would be that, since the various solvents differ in their hydrogen bonding properties, differences in the coupling between the metal amines and the solvent leads to solvent dependent rates of nonradiative deactivation to the ground state. The competitive deactivation pathway leading to ligand displacement would therefore not need to be

influenced by the solvent medium to obtain differences in Φ_{TOT} .

Summary

The results presented here demonstrate that systemic parameters (ligand substituents, solvent, temperature, etc.) can be used to tune the photochemical properties of the $\text{Ru}(\text{NH}_3)_5\text{L}^{2+}$ complexes. The perturbations introduced by changing one of these parameters are the result of several features, but the most prominent of these appears to be the nature of the lowest energy excited states. Thus, the photochemical behaviors in solution can be divided roughly into two categories: (a) complexes having a LF state as the lowest energy excited state and displaying significant photolability and (b) complexes having a lowest energy MLCT state and therefore being much less reactive toward ligand photosubstitution but (in some cases) active toward photoredox processes.¹⁷ The role of solvent is severalfold but a major effect relates to the sensitivity of MLCT state energies to the solvent environment coupled with the insensitivity of LF state energies to the solvent. Thus, in certain cases, *for a complex where the lowest energy MLCT state and the lowest energy LF state have similar energies, changes in the solvent alone may be sufficient to reverse the order of these states.*

Although the observations reported here are for one series of closely related complexes, the view that subtle ligand modifications may have significant effects on photoactivity has broader implications. In certain cases, such modifications may merely reflect changes in the various deactivation pathways available to reactive excited states; however, the cases where the largest effects may be realized are those where excited states of different orbital parentage have comparable energies within the excited state manifold, especially at the lowest energy range of this manifold.

Acknowledgments. This research was supported by the National Science Foundation (GP-36634-X, CHE76-00601). We thank the Matthey Bishop Co. for a loan of the ruthenium used in this study, and Professor R. J. Watts for much helpful and stimulating discussion.

References and Notes

- (1) (a) Presented in part at the 1975 Inorganic Chemistry Symposium, Athens, Ga., Jan 1975, and at the VIIIth International Conference on Photochemistry, Edmonton, Canada, Aug 1975; (b) A preliminary communication describing this work in part is G. Malouf and P. C. Ford, *J. Am. Chem. Soc.*, **96**, 601 (1974).
- (2) Camille and Henry Dreyfus Foundation Teacher Scholar, 1971-1976.
- (3) P. C. Ford, D. H. Stuermer, and D. P. McDonald, *J. Am. Chem. Soc.*, **91**, 6209 (1969).
- (4) P. C. Ford, D. A. Chaisson, and D. H. Stuermer, *Chem. Commun.*, 530 (1971).
- (5) D. A. Chaisson, R. E. Hintze, D. H. Stuermer, J. D. Petersen, D. P. McDonald, and P. C. Ford, *J. Am. Chem. Soc.*, **94**, 6665 (1972).
- (6) P. C. Ford, J. D. Petersen, and R. E. Hintze, *Coord. Chem. Rev.*, **14**, 67 (1974).
- (7) R. E. Hintze, Ph.D. Dissertation, University of California, Santa Barbara, 1974.
- (8) R. E. Hintze and P. C. Ford, *J. Am. Chem. Soc.*, **97**, 2664 (1975).
- (9) R. E. Hintze and P. C. Ford, *Inorg. Chem.*, **14**, 1211 (1975).
- (10) P. C. Ford, D. P. Rudd, R. Gaunder, and H. Taube, *J. Am. Chem. Soc.*, **90**, 1187 (1968).
- (11) (a) J. Bjerrum, A. W. Adamson, and O. Bostrup, *Acta Chem. Scand.*, **10**, 329 (1956); (b) T. Matsubara and P. C. Ford, unpublished results for $\text{Ru}(\text{II})$ and $\text{Rh}(\text{III})$ ammine complexes; (c) K. Nakamaru, K. Jin, A. Tazawa, and M. Kanno, *Bull. Chem. Soc. Jpn.*, **48**, 3486 (1975).
- (12) (a) J. D. Petersen, R. J. Watts, and P. C. Ford, *J. Am. Chem. Soc.*, **98**, 3188 (1976); (b) F. Nordmeyer and H. Taube, *ibid.*, **90**, 1162 (1968).
- (13) R. J. Watts and G. A. Crosby, *J. Am. Chem. Soc.*, **94**, 2606 (1972).
- (14) (a) V. Balzani, L. Moggi, M. F. Manfrin, F. Bolletta, and M. Glerin, *Science*, **189**, 852 (1975); (b) G. Sprintschnick, H. W. Sprintschnick, P. P. Kirsch, and D. G. Whitten, *J. Am. Chem. Soc.*, **98**, 2337 (1976).
- (15) K. Schofield, "Hetero Aromatic Nitrogen Compounds", Plenum Press, New York, N.Y., 1967.
- (16) (a) A similar model has been proposed^{16b} to explain the photochemical reactions of the substituted pyridine complexes of pentacarbonyl tungsten(0), $\text{W}(\text{CO})_5\text{py-X}$. In this case, luminescence data supported the view that, while MLCT* energies are markedly dependent on the nature of the pyridine substituent, LF* energies are not; (b) M. S. Wrighton, H. B. Abrahamson, and D. L. Morse, *J. Am. Chem. Soc.*, **98**, 4105 (1976).

- (17) (a) V. A. Durante and P. C. Ford, *J. Am. Chem. Soc.*, **97**, 6898 (1975); (b) The active species in the photoredox process is the binuclear ion $\text{Ru}(\text{NH}_3)_5(\mu\text{-pyrazine})\text{Cu}^{4+}$ which is also unreactive with regard to photo-substitution.
- (18) G. A. Crosby, K. W. Hipps, and W. H. Elfring, *J. Am. Chem. Soc.*, **96**, 629 (1974).
- (19) R. J. Watts, T. P. White, and B. C. Griffith, *J. Am. Chem. Soc.*, **97**, 6914 (1975).
- (20) M. Wrighton, H. B. Gray, and G. S. Hammond, *Mol. Photochem.*, **5**, 165 (1973).
- (21) (a) H. Saito, J. Fujita, and K. Saito, *Bull. Chem. Soc. Jpn.*, **41**, 863 (1968); (b) J. Burgess, *J. Organomet. Chem.*, **19**, 218 (1969).
- (22) C. K. Wong and A. D. Kirk, *Can. J. Chem.*, **54**, 3794 (1976).
- (23) J. F. Endicott, G. J. Ferraudi, and J. R. Barber, *J. Phys. Chem.*, **79**, 630 (1975).
- (24) S. Sakuraba, S. Mimura, and R. Matsushima, *Bull. Chem. Soc. Jpn.*, **46**, 2784 (1973).
- (25) S. T. Spees and A. W. Adamson, *Inorg. Chem.*, **1**, 531 (1962).
- (26) Ballardini, G. Varani, L. Moggi, V. Balzani, K. R. Olsen, F. Scandola, and M. Z. Hoffman, *J. Am. Chem. Soc.*, **97**, 728 (1975).

The Mechanism of the Photoconversion of α -Phenylcinnamic Esters into 9,10-Dihydrophenanthrenes

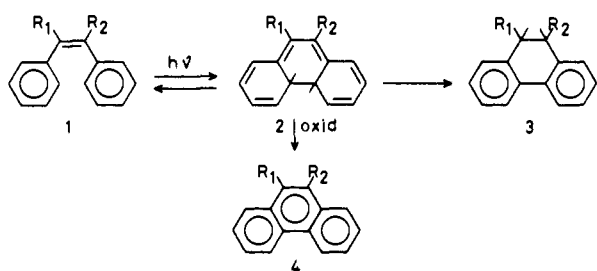
P. H. G. op het Veld and W. H. Laarhoven*

Contribution from the Department of Organic Chemistry, Catholic University, Toernooiveld, Nijmegen, The Netherlands. Received April 4, 1977

Abstract: The mechanism of the formation of a 9,10-dihydrophenanthrene derivative (**3g**) from methyl α -phenylcinnamate (**1g**) is clarified by demonstrating that the 4a,4b-dihydrophenanthrene derivative (**2g**) is an intermediate. It is formed by photocyclization of the parent compound. Only in a protic solvent this intermediate undergoes a prototropic shift leading to a 4a,9-dihydrophenanthrene derivative (**9g**). This compound is converted into the end product **3g** by a radical process. A necessary condition for the formation of a 9,10-dihydrophenanthrene from a stilbene is the presence of an enolizable group at the double bond of the stilbene.

It has been known for over 25 years that stilbenes undergo photochemical cyclodehydrogenations under oxidative conditions to phenanthrenes.¹ More recently, it has been shown^{2,3} that the first step in this reaction is the cyclization from the S_1 state of a *cis*-stilbene (**1**) to a *trans*-4a,4b-dihydrophenanthrene (**2**) (Scheme I). The subsequent dehydrogenation **2** \rightarrow **4** can occur in several ways.⁴

Scheme I



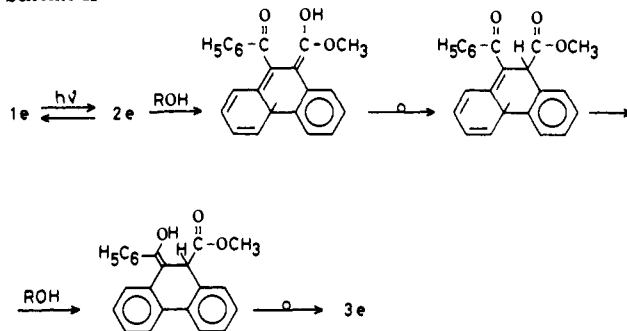
- a) $R_1 = R_2 = \text{CN}$
 b) $R_1 R_2 = \text{CO-O-CO}$
 c) $R_1 R_2 = \text{CO-NH-CO}$
 d) $R_1 = \text{CO-C}_6\text{H}_5$; $R_2 = \text{COOH}$
 e) $R_1 = \text{CO-C}_6\text{H}_5$; $R_2 = \text{COOCH}_3$
 f) $R_1 R_2 = \text{C}(\text{C}_6\text{H}_5)\text{OH-O-CO}$
 g) $R_1 = \text{H}$; $R_2 = \text{COOCH}_3$
 h) $R_1 = \text{H}$; $R_2 = \text{CN}$

In general, the reaction **1** \rightarrow **2** is completely reversible under nonoxidative conditions; **2** can undergo both thermal and photochemical ring opening^{4,5} to *cis*-**1**. In a few cases, however, it was found that irradiation of a stilbene in the absence of an oxidant yielded a 9,10-dihydrophenanthrene (**3**). Thus, Sargent and Timmons⁶ reported that the stilbenes **1a-c** which possess two electron-withdrawing substituents on the double bond yield the products **3a-c** on irradiation under nonoxidative conditions. Irradiation of stilbene, triphenylethylene, α -methylstilbene, and α -cyanostilbene under the same conditions gave only *cis*-*trans* isomerization. The authors ascribed the formation of the products **3a-c** to photochemically induced H shifts in the primary formed intermediates **2a-c**.

In 1970 Rio and Hardy obtained the 9,10-dihydrophenan-

threnes **3d-f** on irradiation of the stilbenes (derivatives) **1d-f** in various alcohols or in a mixture of water-pyridine as the solvent, even when the irradiation was carried out in the presence of oxygen.⁷ By performing the reactions in D_2O -pyridine they were able to show that the hydrogen atoms at C_9 and C_{10} in the products **3d-f** were derived from the solvent. On irradiation of the same stilbene derivatives in benzene or chloroform they observed a red coloration of the solution, which was ascribed to the occurrence of the intermediates **2d-f**, but they could not isolate 9,10-dihydrophenanthrenes from the irradiation mixtures. Rio and Hardy suggested a mechanism wherein prototropic shifts are responsible for the isomerization **2** \rightarrow **3** (see Scheme II). Consequently they state that com-

Scheme II



pounds with only one electron-withdrawing substituent on the olefinic bond may not be expected to give 9,10-dihydrophenanthrenes. Such compounds will only give rise to *cis*-*trans* isomerization. Ichimura and Watanabe⁸ used a similar mechanism in their study of the pH dependence of the photocyclization **1a** \rightarrow **3a**.

In 1971 Srinivasan and Hsu⁹ reported the first example of a photocyclization wherein a stilbene derivative having only one electron-withdrawing substituent on the olefinic bond gave a 9,10-dihydrophenanthrene as the product. On irradiation of